Journal of Electronic Imaging

SPIEDigitalLibrary.org/jei

Image enhancement approach using the just-noticeable-difference model of the human visual system

Chang-Hsing Lee
Pei-Ying Lin
Ling-Hwei Chen
Wei-Kang Wang

Image enhancement approach using the just-noticeable-difference model of the human visual system

Chang-Hsing Lee
Chung Hua University
Department of Computer Science and Information Engineering
707, Section 2, WuFu Road
Hsinchu, Taiwan 30012

Pei-Ying Lin
Ling-Hwei Chen
Wei-Kang Wang
National Chiao Tung University
Institute of Multimedia Engineering
1001 University Road
Hsinchu, Taiwan 30010
E-mail: lhchen@cc.nctu.edu.tw

Abstract. *The low-contrast images taken by digital cameras or camera phones are not always satisfactory due to the limitation of the capturing devices or improper illumination/exposure conditions. Conventional image contrast enhancement methods may either fail to produce satisfactory and undistorted images, or they cannot improve every region of interest appropriately, especially faces. In this paper, a histogram equalization (HE) approach exploiting the just-noticeable-difference (JND) model of the human visual system (HVS), denoted by JND-HE, is proposed for generic image contrast enhancement. Further, the proposed JND-HE approach is combined with the exposure correction (EC) method (denoted by JND-HE-EC) for face image enhancement. The proposed JND-HE-EC approach can improve the contrast in face regions and provide proper illumination in the background. Experimental results on both generic images and faces have shown that our proposed approach can produce more pleasing and appealing enhanced images than other methods.*
 [DOI: 10.1117/1.JEI.21.3.033007]

1 Introduction

In recent years, digital cameras and camera phones have been widely used in our daily lives. People may take many unsatisfactory images due to the limitation of the capturing devices or improper illumination/exposure conditions. In addition, the contrast of an image may be greatly affected if the images were taken in bad weather, especially foggy or rainy conditions. The common defects appearing in real-life images include (1) a dark image due to poor illumination, (2) an image with an underexposed background and an overexposed subject, (3) an image with a dark subject and a bright background due to backlighting, and (4) a low-contrast image owing to the influence of fog or moisture. Many software[1,2] or image enhancement methods[3–10] were developed to cope with these problems. In general, these methods can be classified into three categories: histogram-based methods,[3–6] transform-based methods,[3,7,8] and exposure-based methods.[9,10]

Histogram equalization (HE),[3] which is based on the adjustment of histograms, is the best-known and most widely used technique for image contrast enhancement. HE uses a nonlinear mapping function to produce an image with a histogram approximating a uniform distribution. This method will spread out the values that occur more frequently and compress those values that occur less frequently to get an image of higher contrast. However, HE fails to produce satisfactory pictures owing to three common drawbacks:[11] (1) false contour [see Fig. 1(b)]; (2) amplified noises [see Fig. 2(b)]; and (3) washed-out appearance [see Fig. 3(b)]. Several advanced HE methods[4–6] have been proposed to improve the image contrast. The global HE methods, such as bi-HE[4] and dualistic subimage HE,[5] first divide the histogram into two parts and then independently apply HE on each subhistogram. These methods can preserve the original brightness to some extent, which is essential for consumer electronic products, but they may also produce unpleasant artifacts for some images. Pizer et al.[6] proposed a local HE method called adaptive HE. First, an image is divided into several blocks, and then HE is applied to each block. Finally, the enhanced image blocks are fused together using bilinear interpolation. The main drawback of these HE-based methods is that some regions in the images may be enhanced excessively.

For transform-based methods,[3,7,8] a transformation function (e.g., the power-law transformation function or logarithm transformation function) is defined to map an input luminance value into an output one. These methods were widely provided in many commercial devices and

Paper 11195 received Jul. 22, 2011; revised manuscript received Apr. 19, 2012; accepted for publication Jun. 11, 2012; published online Jul. 13, 2012.

0091-3286/2012/$25.00 © 2012 SPIE and IS&T

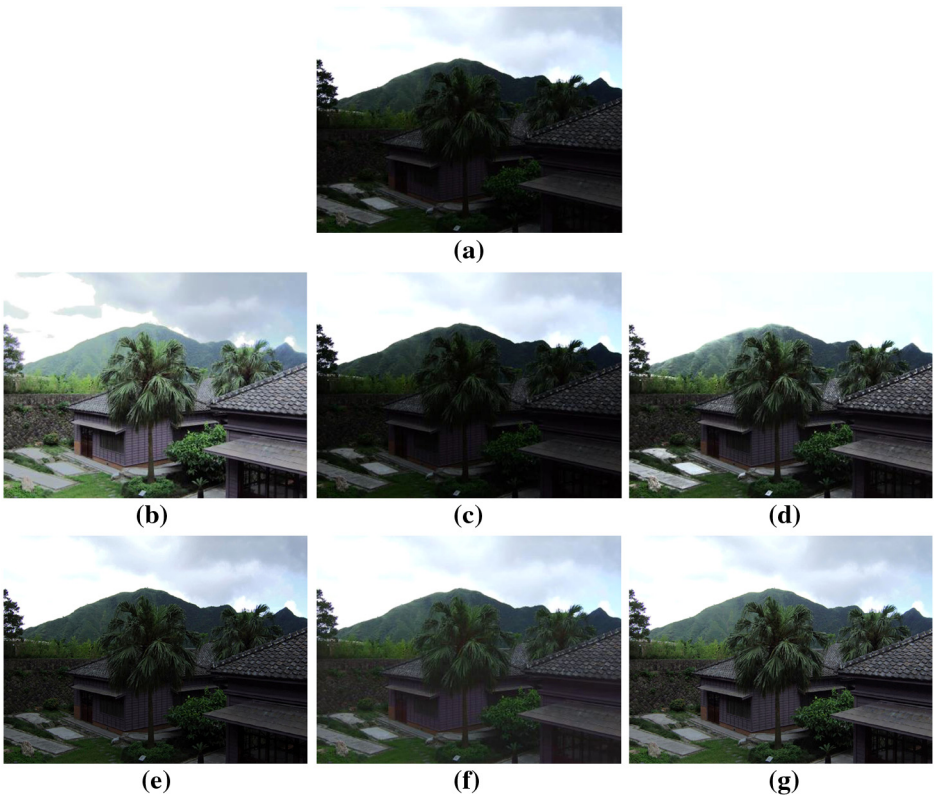

Fig. 1 Comparison of different enhancement approaches on an image with overexposed and underexposed regions. (a) Original image; (b) HE-enhanced image; (c) Picasa software—enhanced image; (d) EC-enhanced image; (e) LCC-enhanced image; (f) SC-enhanced image; and (g) JND-HE—enhanced image.

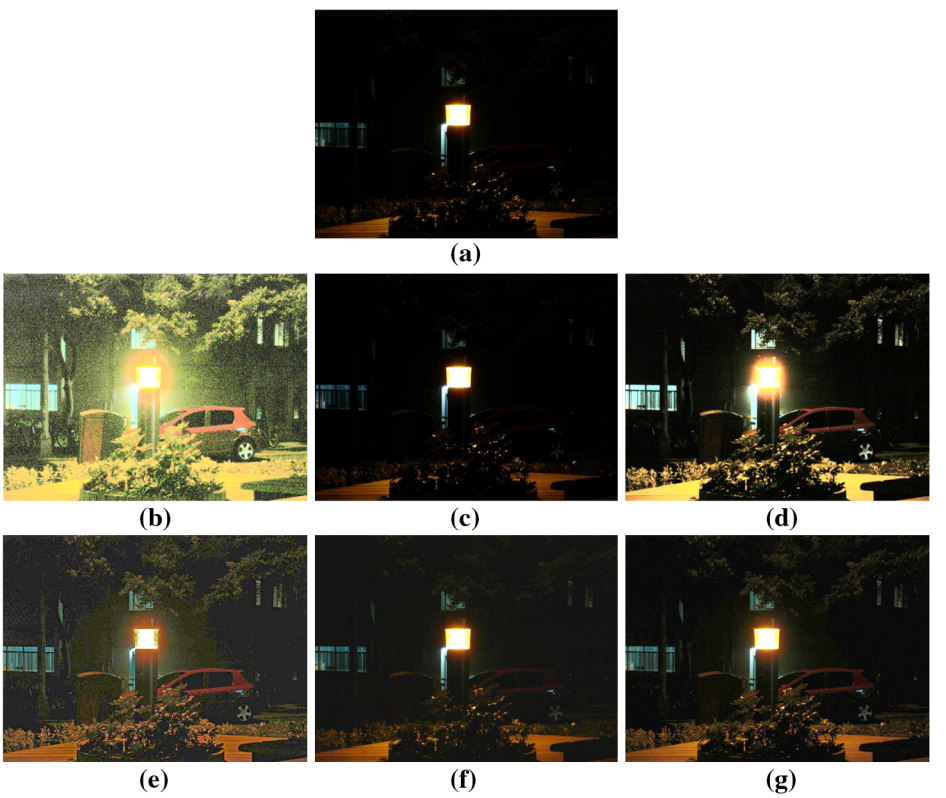

Fig. 2 Comparison of different enhancement approaches on a dark scene. (a) Original image; (b) HE-enhanced image; (c) Picasa software-enhanced image; (d) EC-enhanced image; (e) LCC-enhanced image; (f) SC-enhanced image; (g) JND-HE-enhanced image.

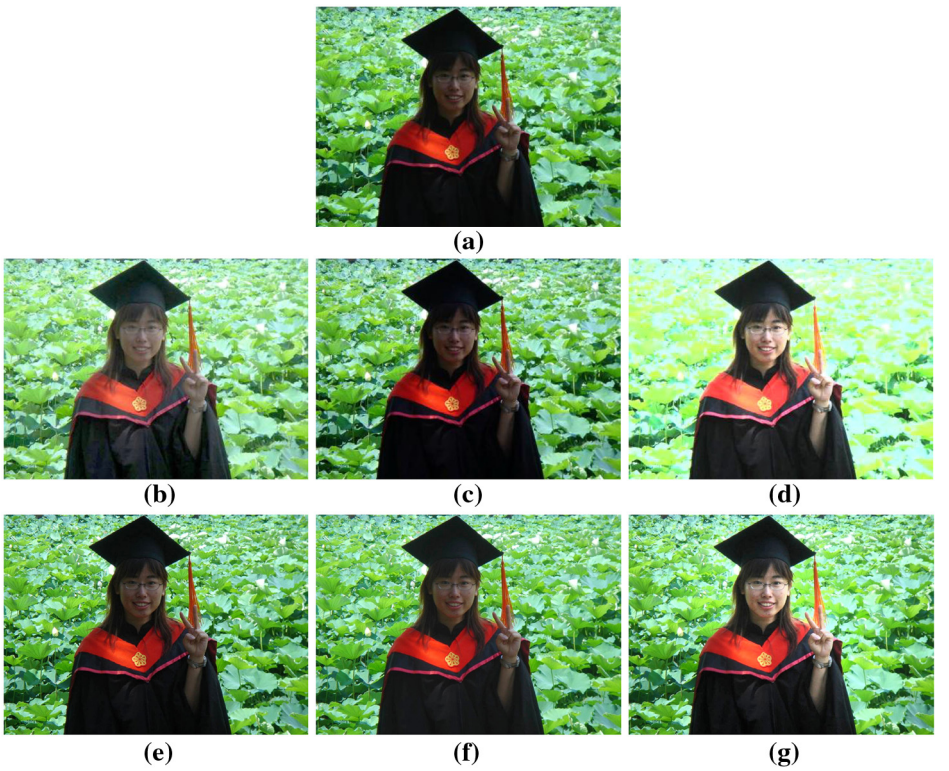

Fig. 3 Comparison of different enhancement approaches on a face image taken under backlight conditions. (a) Original image; (b) HE-enhanced image; (c) Picasa software—enhanced image; (d) EC-enhanced image; (e) LCC-enhanced image; (f) SC-enhanced image; and (g) JND-HE-EC-enhanced image.

software.[3] However, some device-dependent parameters need to be determined in advance. Transform-based methods generally can produce a properly enhanced image for either underexposed images or overexposed images by selecting appropriate parameters.[3] However, if an image has both underexposed and overexposed regions, transform-based methods fail to produce appropriate contrast on both regions. Moroney[7] proposed an enhancement approach based on pixel-wise gamma correction with a nonlinear masking. The gamma correction of each pixel depends on the values of its neighboring pixels. However, it may produce halo effects near the edges. Thus, Schettini et al.[8] proposed the local contrast correction method, which is based on a local and image-dependent gamma correction with parameters determined automatically by image statistics analysis, to enhance overexposed and underexposed regions simultaneously. The bilateral filter is used as the mask for gamma correction in an attempt to reduce halo effects. Finally, a contrast enhancement module consisting of stretching, clipping, and saturation preserving is developed to increase the contrast. Although overexposed and underexposed regions can be well enhanced, the global contrast of the whole image also was reduced.

Exposure-based methods[9,10] tried to adjust the exposure level of an image using a mapping function between the light values and the pixel values of interested objects. Battiato et al.[9] proposed a content-dependent exposure correction approach using the camera response curve to adjust the exposure levels. The algorithm first identifies the visually relevant regions and calculates the offset between the average luminance value of visually relevant regions and the desired target luminance value. The offset value was then employed to modify the luminance value of every pixel in the image. Since this approach was specifically designed for interested regions, it can produce pleasing results in interested regions, but it may lead to poorer illumination in other regions [see Fig. 3(d)]. Safonov et al.[10] developed an enhancement method for global and local correction of various exposure defects. Their approach is based on contrast stretching and alpha-blending of both the brightness of the original image and the estimated reflectance.

In this paper, enhancement approaches for real-life images with and without face regions will be proposed. For generic images, an HE approach exploiting the just-noticeable-difference (JND) model of the human visual system (HVS), denoted by JND-HE, will be proposed. For face image enhancement, the proposed JND-HE approach will be combined with the exposure correction (EC) method,[9] denoted by JND-HE-EC, to produce a pleasing image with appropriate contrast in background regions and proper illumination in face regions.

In the next section, we will describe the proposed JND-HE image enhancement approach. Section 3 gives the proposed JND-HE-EC face image enhancement approach. Some experimental results and performance comparisons will be shown in Sec. 4. Finally, Sec. 5 gives a conclusion and a discussion of the future prospects of this work.

2 Proposed Generic Image Enhancement Approach

In this paper, HE will be integrated with the JND model of the HVS for generic image enhancement. Before describing

the proposed approach, we will first give a brief review of HE and analyze its defects.

2.1 *Histogram Equalization*

HE[3] tries to increase the contrast of an image using a nonlinear mapping function to make the enhanced histogram approximate a uniform distribution. For color images, HE is typically applied to the histogram of the luminance value, Y, converted from the red, green, and blue color values using the following conversion function:

$$Y(x,y) = 0.299 \cdot R(x,y) + 0.587 \cdot G(x,y) + 0.114 \cdot B(x,y), \quad (1)$$

where $R(x,y)$, $G(x,y)$, and $B(x,y)$ denote the red, green, and blue color values of a pixel located at (x,y). Let variable k represent the luminance value in the interval (0, 255). Then, the occurrence probability of the luminance value k, $p(k)$, in an image is defined as follows:

$$p(k) = \frac{n_k}{N}, \quad (2)$$

where N is the total number of pixels in the image, and n_k is the number of pixels with luminance value k. Then, the nonlinear transformation function T that maps a luminance value k into a reconstructed luminance value s is given by:

$$s = T(k) = 255 \sum_{i=0}^{k} p(i) = 255 \sum_{i=0}^{k} \frac{n_i}{N}. \quad (3)$$

From Eq. (3), the difference between the enhanced values of k and $k+r$, denoted by $T(k)$ and $T(k+r)$, can be represented as follows:

$$d_E(k,r) = T(k+r) - T(k) = 255 \times \sum_{i=0}^{k+r} p(i) - 255 \times \sum_{i=0}^{k} p(i) = 255 \times \sum_{i=k+1}^{k+r} p(i). \quad (4)$$

Thus, the gap $d_E(k,r)$ between the enhanced values $T(k)$ and $T(k+r)$ is directly proportional to the accumulative probability between $k+1$ and $k+1$. If some $p(i)$, for $i \in \{k+1, \ldots, k+r\}$, is abnormally large, a larger gap $d_E(k,r)$ can be obtained. As a result, false contours might appear in the enhanced image. Specifically, for a dark image in which most pixels have low luminance values, the contrast-stretching result using HE will excessively enhance the low-luminance part and push the medium-luminance values toward the higher ones. As a result, the noises hidden in the dark regions will be amplified and the whole image exhibits a washed-out appearance. In conclusion, when the histogram of an image has very high peaks at some specific values or concentrates in a small range of levels, HE fails to produce pleasingly enhanced images. To prevent these defects, the JND model of the HVS will be integrated with HE to produce well-enhanced images.

2.2 *The Proposed JND-based Histogram Equalization (JND-HE) Approach*

Typically, an image enhancement method should not only produce high-contrast images, but also prevent the introduction of any noticeable distortion/noise. In the proposed JND-HE approach, we design an evaluation function, based on the JND model of the HVS, to assess whether HE will introduce any noticeable distortion/noise in the enhanced images.

JND is a quantitative measure for distinguishing the luminance change perceived by the HVS. In other words, JND gives the maximum difference of the luminance values that can be perceived by human eyes. In this paper, the JND model proposed by Chou and Li[12] will be employed to design the evaluation function. The perceptual function for evaluating the visibility threshold of the JND model can be described by the following equation:

$$\mathrm{JND}(k) = \begin{cases} T_0[1 - (k/127)^{0.5}] + 3, & k \le 127 \\ \gamma(k - 127) + 3, & \text{otherwise} \end{cases}, \quad (5)$$

where k is the luminance value within (0, 255) and the parameters T_0 and γ depend on the viewing distance between a tester and the monitor. T_0 denotes the visibility threshold when the background gray level is 0, and γ denotes the slope of the line that models the JND visibility threshold function at higher background luminance. In this study, T_0 and γ are set to be 17 and $3/128$, based on the subjective experiments conducted by Chou and Li.[12] Figure 4 shows the visibility threshold for different gray values computed by using Eq. (5). It can be seen that HVS is relatively sensitive to the change of luminance at the medium of the luminance range. In contrast, HVS is less sensitive to the change of luminance for dark or bright regions. In this figure, the smallest visibility threshold is 3 when k is 127.

Note that the visibility threshold evaluated in this study considers only the effect of average background luminance, without taking into account spatial masking (i.e, spatial nonuniformity of the background luminance). In general, if both average background luminance and spatial masking are considered, the evaluated visibility threshold will be larger than that depicted in Fig. 4. However, it is impossible to use the spatial masking concept on the HE approach because HE maps pixels of the same value into identical output values without considering their spatial contexts. Thus, to incorporate the JND model into HE directly, we used only the

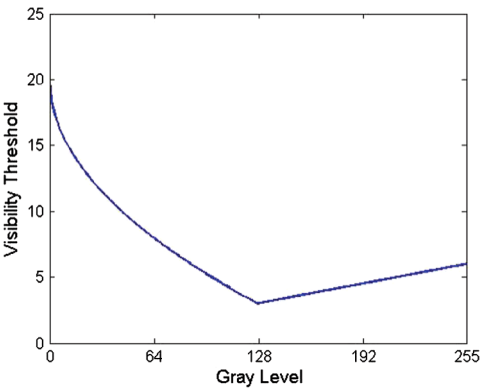

Fig. 4 Visibility threshold JND(k), evaluated for different gray levels.

average background luminance concept to evaluate the visibility threshold.

As shown in Eq. (4), the difference $d_E(k,r)$ between the enhanced values $T(k)$ and $T(k+r)$ of two nearby values k and $k+r$ represents the amplified contrast value resulting from HE. If the difference between k and $k+r$ is smaller than the JND threshold value evaluated on k [that is, $r < \mathrm{JND}(k)$], k and $k+r$ will be indistinguishable by human eyes. To avoid excessive contrast stretching, we have to make sure that $d_E(k,r)$ should also be smaller than the JND threshold value evaluated on $T(k)$, for $0 \le k \le 255$. This constraint will ensure that for every two nearby luminance values, the corresponding amplified contrast value will be indistinguishable to human eyes. Therefore, we represent the evaluation function in the following form:

$$d_E(k,r) < \mathrm{JND}[T(k)] \ \forall\ k, 0 \le k \le 255, 1 \le r \le r_{\max}, \quad (6)$$

or equivalently,

$$\sum_{i=k+1}^{k+r} p(i) < \mathrm{JND}[T(k)]/255 \ \forall\ k, 0 \le k \le 255, 1 \le r \le r_{\max} \quad (7)$$

calculated by using Eq. (4), where $r_{\max}$ is defined as the smallest visibility threshold evaluated for all luminance values; that is,

$$r_{\max} = \min_{0 \le k \le 255} \mathrm{JND}(k). \quad (8)$$

In fact, $r_{\max} = 3$, calculated by using Eq. (5). This JND evaluation function can help to determine whether smooth regions in the enhanced image will exhibit any perceived distortion or not. In this paper, we will use the evaluation function to determine whether HE can be directly employed for image enhancement. If the JND evaluation function is satisfied for every luminance value k, HE will be used to obtain an enhanced image without producing any artifacts. Otherwise, the enhanced result will definitely exhibit some noticeable artifacts. Thus, a histogram curve adjustment procedure will be designed to generate a qualified histogram curve before HE. Figure 5 shows the flowchart of the proposed JND-HE approach.

2.3 *Histogram Curve Adjustment*

In general, it is more probable that the JND evaluation function will be satisfied if the peak values in the histogram are attenuated. Based on this idea, we remove the highest peaks in the histogram and uniformly redistribute the corresponding eliminated values among all histogram components. This adjustment will spread the excessively concentrated probabilities at some certain histogram components over the other ones with lower probabilities. The procedure for histogram curve adjustment consists of three stages: sorting, shifting, and redistribution. A detailed description of these three stages is given next.

2.3.1 *Sorting*

The histogram component, $p(k)$, represents the occurrence probability of luminance value k, $0 \le k \le 255$. Let L denote the number of histogram components, and let n denote the iteration number of the histogram curve adjustment process conducted so far, with $n = 1$ initially. First, the histogram is sorted in descending order. Let index i denote the index of the ith sorted component. Thus, index(1) and index(L) are the indices having the largest and the smallest probability values, respectively, among all histogram components.

2.3.2 *Shifting*

First, reset the n largest component values to 0. For example, if $n = 2$, the component values corresponding to indices of index(1) and index(2) are set to 0. That is, $p[\mathrm{index}(1)] = p[\mathrm{index}(2)] = 0$. Next, shift each sorted histogram component by n values. That is, each sorted component value will be replaced with the next nth sorted component value and the last n values are reset to 0:

$$p_n^{\mathrm{shift}}[\mathrm{index}(i)] = \begin{cases} p[\mathrm{index}(i+n)], & 1 \le i \le L-n \\ 0, & \text{otherwise} \end{cases}. \quad (9)$$

2.3.3 *Redistribution*

Since some histogram component values are eliminated in the new shifted histogram, the sum of the remaining component values will be less than 1. To deal with this problem, we uniformly redistribute the sum of these eliminated component values to all histogram components using the following equation:

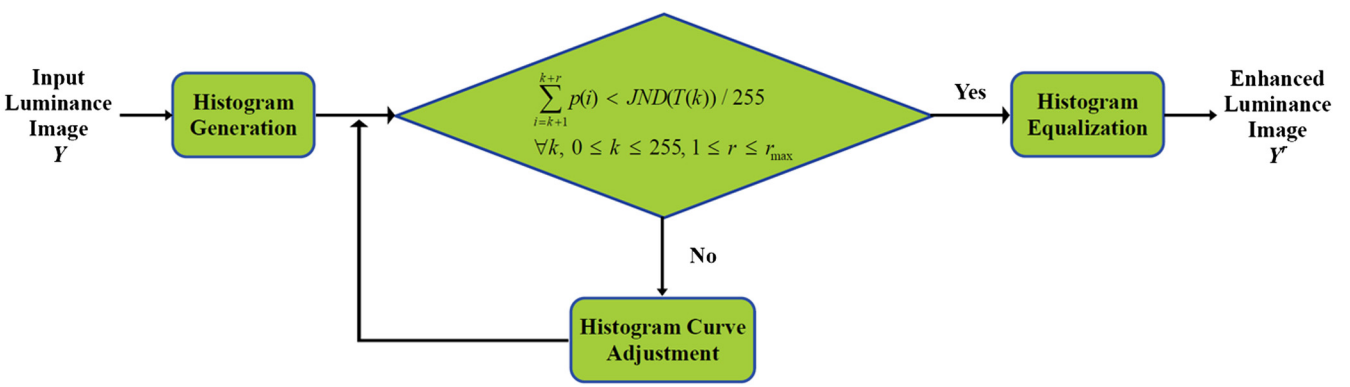

Fig. 5 The flowchart of the proposed JND-HE approach.

$$p_n^{\text{redis}}(i) = p_n^{\text{shift}}(i) + p_{\text{avg}}^{\text{redis}}, \qquad 1 \le i \le L, \tag{10}$$

where $p_{\text{avg}}^{\text{redis}}$ is the average of the eliminated component values given by

$$p_{\text{avg}}^{\text{redis}} = \frac{1}{L}\sum_{i=1}^{n} p[\text{index}(i)]. \tag{11}$$

As a result, the shifted and redistributed histogram will become smoother than the original one. If this histogram satisfies the JND evaluation function defined in Eq. (7), terminate the histogram adjustment procedure and apply the HE mapping function [Eq. (3)] on this new histogram to get the enhanced image. Otherwise, set $n = n + 1$ and perform the shifting and redistribution operation repeatedly until a qualified histogram is obtained. It should be noted that the larger the value of the iteration number (n) is, the smoother the histogram is. This is because as n increases, more histogram peaks will be eliminated. Hence, a qualified histogram that satisfies the JND evaluation function finally can be obtained after a number of iterations. Table 1 gives an example of the histogram curve adjustment procedure with eight histogram components. We can see from this that the redistributed histogram is smoother than the original one.

2.4 *Prevention of Over-adjustment*

By repeating the histogram adjustment procedure described above, we can get a qualified image in which no visible distortion will appear in the enhanced image. However, a smoother histogram curve will deteriorate the contrast-stretching ability of HE. In order to avoid this over-adjustment phenomenon, an interpolation histogram can be derived using a weighted average of the shifted histograms obtained in the current iteration and the previous iteration:

$$p_n^{\text{int}}[\text{index}(i)] = \omega p_n^{\text{shift}}[\text{index}(i)] + (1-\omega)p_{n-1}^{\text{shift}}[\text{index}(i)], 1 \le i \le L, \tag{12}$$

where $0 \le \omega \le 1$. In this paper, we set $p_0^{\text{shift}}[\text{index}(i)] = p[\text{index}(i)]$, $1 \le i \le L$. Note that the sum of all component values in the interpolation histogram is not equal to 1. Thus, the averaged difference will be evenly added to all interpolation histogram components to get the corrected interpolation histogram components:

$$p_n^{\text{cint}}[\text{index}(i)] = p_n^{\text{int}}[\text{index}(i)] + p_{\text{avg}}^{\text{int}}, 1 \le i \le L, \tag{13}$$

where $p_{\text{avg}}^{\text{int}}$ is the averaged difference given by

$$p_{\text{avg}}^{\text{int}} = \frac{1}{L}\left\{1 - \sum_{i=1}^{L} p_n^{\text{int}}[\text{index}(i)]\right\}. \tag{14}$$

In this paper, the binary search algorithm will be used to find the smallest interpolation parameter ω between 0 and 1 with which the interpolation histogram will satisfy the JND evaluation function. Finally, HE will be applied to the corrected interpolation histogram to obtain the enhanced image.

An example showing the results of applying the histogram adjustment procedure is shown in Fig. 6. First, an input dark scene image is shown in Fig. 6(a). Using Eq. (7) as the JND evaluation function for $r = 1$, we can find that its histogram is not qualified. Thus, the histogram curve adjustment procedure will be conducted iteratively. By repeatedly applying the shifting and redistribution operations to the original histogram, we can find a qualified histogram after five iterations ($n = 5$). Figure 6(b) through 6(g) shows the enhanced results for different numbers of adjustment operations ($0 \le n \le 5$). Note that the case for $n = 0$ denotes that no histogram curve adjustment operation is conducted before HE. It can be seen that the noises in the background are gradually attenuated and the overexposed areas are greatly improved. Figure 6(h) is the final enhanced image obtained by interpolating the histograms corresponding to $n = 4$ and $n = 5$ with $\alpha = 0.6$. Figure 6(i) compares the original histogram and the adjusted histogram. We can see that the high peaks in the histogram are greatly attenuated, whereas the other histogram components are increased slightly and evenly.

Table 1 An example illustrating the histogram curve adjustment operation for $n = 1$, given eight histogram components.

Original histogram	Sorted index	Sorted histogram	Shifted histogram	Redistributed histogram $p_{\text{avg}}^{\text{redis}} = 0.400/8 = 0.05$
$p(0) = 0.250$	$\text{index}(1) = 1$	$p[\text{index}(1)] = 0.400$	$p[\text{index}(1)] = 0.250$	$p[\text{index}(1)] = 0.250 + 0.05 = 0.300$
$p(1) = 0.400$	$\text{index}(2) = 0$	$p[\text{index}(2)] = 0.250$	$p[\text{index}(2)] = 0.125$	$p[\text{index}(2)] = 0.125 + 0.05 = 0.175$
$p(2) = 0.125$	$\text{index}(3) = 2$	$p[\text{index}(3)] = 0.125$	$p[\text{index}(3)] = 0.100$	$p[\text{index}(3)] = 0.100 + 0.05 = 0.150$
$p(3) = 0.045$	$\text{index}(4) = 7$	$p[\text{index}(4)] = 0.100$	$P[\text{index}(4)] = 0.045$	$p[\text{index}(4)] = 0.045 + 0.05 = 0.095$
$p(4) = 0.030$	$\text{index}(5) = 3$	$p[\text{index}(5)] = 0.045$	$P[\text{index}(5)] = 0.030$	$p[\text{index}(5)] = 0.030 + 0.05 = 0.080$
$p(5) = 0.020$	$\text{index}(6) = 4$	$p[\text{index}(5)] = 0.030$	$p[\text{index}(5)] = 0.030$	$p[\text{index}(5)] = 0.030 + 0.05 = 0.080$
$p(6) = 0.030$	$\text{index}(7) = 6$	$p[\text{index}(7)] = 0.030$	$p[\text{index}(7)] = 0.020$	$p[\text{index}(7)] = 0.020 + 0.05 = 0.070$
$p(7) = 0.100$	$\text{index}(8) = 5$	$p[\text{index}(8)] = 0.020$	$p[\text{index}(8)] = 0.000$	$p[\text{index}(8)] = 0.000 + 0.05 = 0.050$

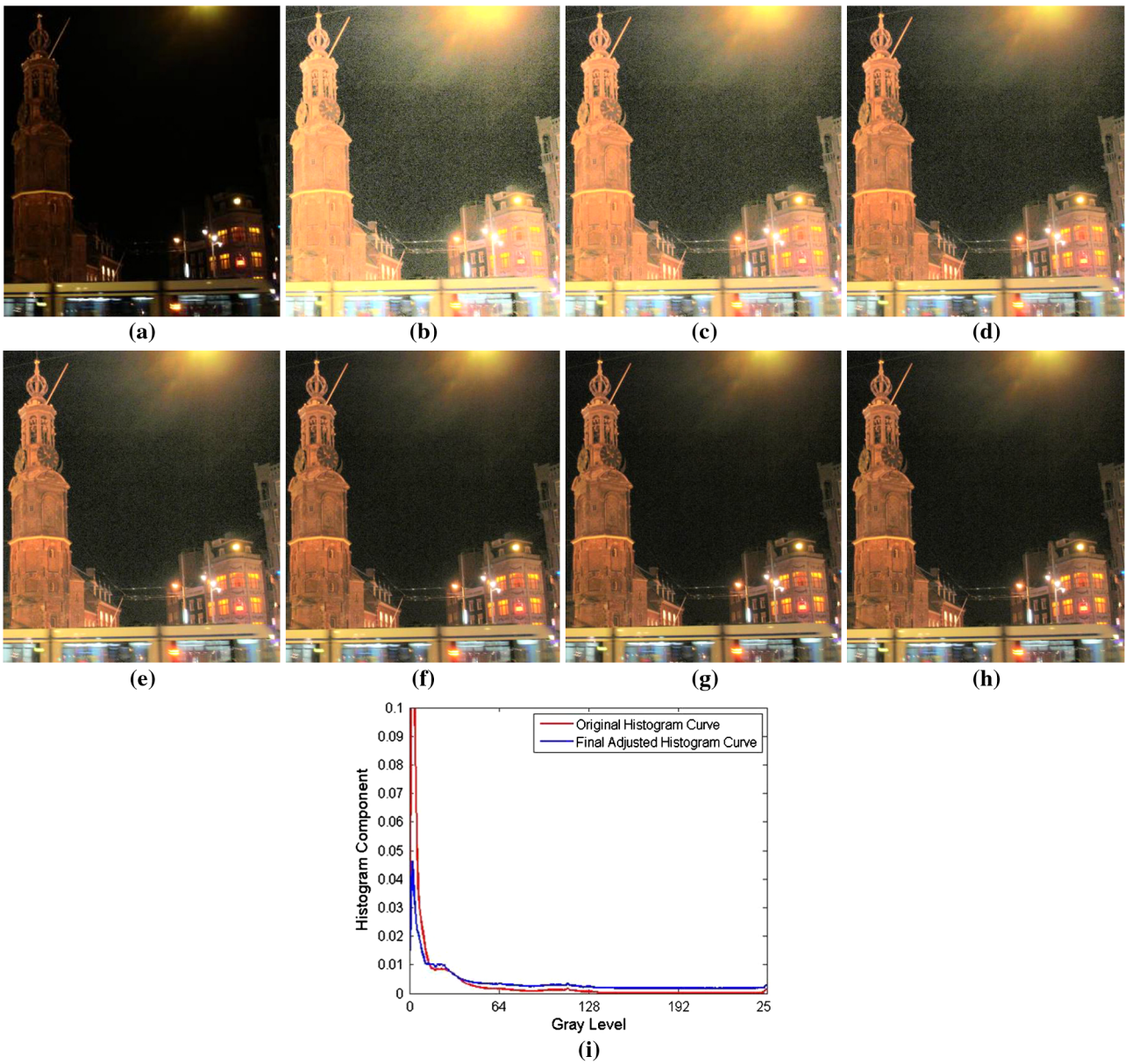

Fig. 6 An example showing the results of applying the histogram adjustment procedure for different numbers of adjustment operations (n) using the JND evaluation function for $r = 1$. (a) Original dark scene image; (b) enhanced image for $n = 0$; (c) enhanced image for $n = 1$; (d) enhanced image for $n = 2$; (e) enhanced image for $n = 3$; (f) enhanced image for $n = 4$; (g) enhanced image for $n = 5$; (h) the final enhanced image; (i) the original and final adjusted histogram curves.

2.5 *Linear Image Fusion*

Figure 7 compares the enhanced images using the JND evaluation function for different values of r. Note that the parameter r determines how many histogram components will be accumulated in the JND evaluation function defined in Eq. (7). The larger the parameter r is, the stricter the JND evaluation function is. That is, a large r value will eliminate a larger number of histogram peaks in the histogram curve adjustment process. As a result, the adjusted histogram becomes flatter, and thus, the subsequent HE will not modify the input image too much. It can be seen that for $r = 1$, the noise around the streetlight is amplified slightly [see Fig. 7(a)]. We can also see that for $r = 3$, the noise is attenuated [see Fig. 7(c)], whereas the contrast is reduced as well (see the red car). In this study, we will perform a linear image fusion on the enhanced images for different r values by using pixel-by-pixel averaging to yield a fused image with low noise and better contrast. Let $Y_1(x, y)$, $Y_2(x, y)$, and $Y_3(x, y)$ denote the enhanced luminance images for $r = 1$, 2, and 3, respectively. The fused image can be obtained using the following equation:

$$Y_{\text{JND-HE}}(x, y) = \frac{1}{3} Y_1(x, y) + \frac{1}{3} Y_2(x, y) + \frac{1}{3} Y_3(x, y). \quad (15)$$

Figure 7(d) shows the fused image. It can be seen that the fused image provides a better trade-off between low noise and high contrast.

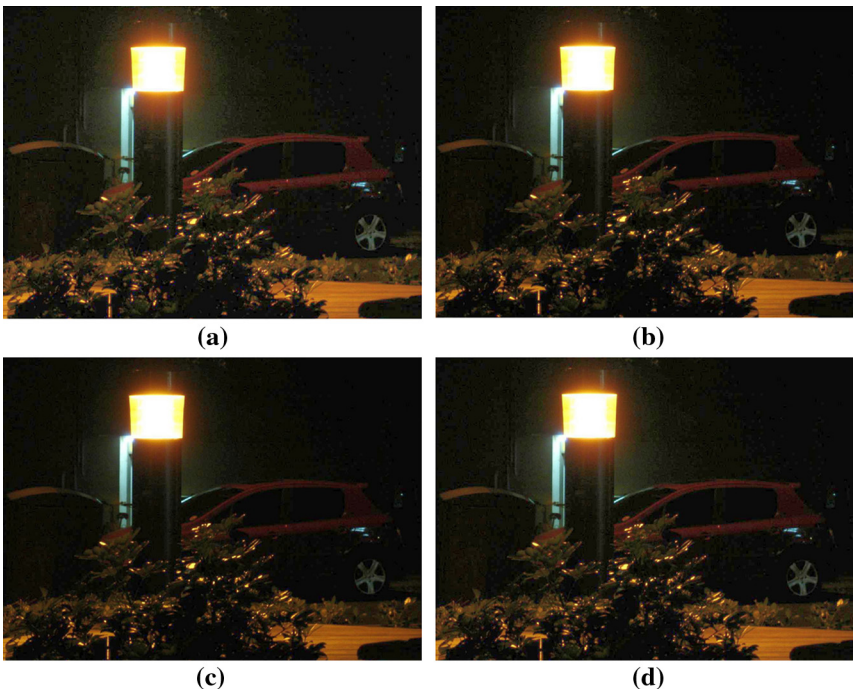

Fig. 7 Comparison of the enhanced images using the JND evaluation function for different values of r. (a) $r = 1$; (b) $r = 2$; (c) $r = 3$; and (d) the fused image.

2.6 *Color Reconstruction*

After obtaining the enhanced luminance value $Y_{\text{JND-HE}}(x, y)$, the R, G, B color values will be reconstructed by using the following formula to prevent relevant hue shift and color de-saturation:[13]

$$R^r(x,y) = \frac{1}{2}\left\{\frac{Y_{\text{JND-HE}}(x,y)}{Y(x,y)}[R(x,y)+Y(x,y)] + R(x,y) - Y(x,y)\right\}, \quad (16)$$

$$G^r(x,y) = \frac{1}{2}\left\{\frac{Y_{\text{JND-HE}}(x,y)}{Y(x,y)}[G(x,y)+Y(x,y)] + G(x,y) - Y(x,y)\right\}, \quad (17)$$

$$B^r(x,y) = \frac{1}{2}\left\{\frac{Y_{\text{JND-HE}}(x,y)}{Y(x,y)}[B(x,y)+Y(x,y)] + B(x,y) - Y(x,y)\right\}, \quad (18)$$

3 The Proposed Face Image Enhancement Method

In real-life images, the face regions are usually the most relevant parts in terms of human perception. Conventional image enhancement methods[3–8,10,11] do not specifically treat face regions in improper illumination/exposure environments. Hence, these enhancement techniques fail to offer proper contrast or alleviate improper illumination in face regions. As a result, face regions will exhibit a washed-out appearance or unnatural look [see Fig. 8(b), 8(c), and 8(e)]. On the other hand, some enhancement techniques[9,14,15] were particularly designed to enhance the face regions. From Fig. 8(d), we can see that the EC method[9] can produce a satisfying exposure in face regions, whereas it might cause improper illumination in background regions. Therefore, a face image enhancement approach, which combines our proposed JND-HE approach with the EC method, denoted by JND-HE-EC, will be designed to enhance both face and nonface regions simultaneously. First, according to the mean luminance value of all detected face skin pixels, EC is employed to obtain an enhanced image, denoted by Y_{EC}. Meanwhile, JND-HE is used to get another enhanced image, denoted by $Y_{\text{JND-HE}}$. Finally, a distance map is constructed to fuse together Y_{EC} and $Y_{\text{JND-HE}}$ to obtain the final enhanced image $Y_{\text{JND-HE}}$. The flowchart of the proposed JND-HE-EC approach for face image enhancement is shown in Fig. 9.

3.1 *Face Skin Pixel Identification*

First, the face regions in the input image are detected using the face detection framework proposed by Viola and Jones,[16,17] which can quickly and robustly detect frontal, upright faces. Then, the skin pixels in the detected face regions are identified. In this paper, the skin locus model,[18] which is robust under multiple lighting sources or varying illumination environments, is employed to detect all possible skin pixels. This model is based on the (r, g)-plane obtained by normalizing the color values (R, G, B) of each pixel, given by $r = R/(R+G+B)$ and $g = G/(R+G+B)$. From the statistical analysis on the color distribution of skin pixels, Soriano et al. found that in the (r, g)-plane, the color values of skin pixels tend to cluster together in a shell-shaped area,[18] which is defined by a pair of quadratic functions denoting its upper curve and lower curve:

$$g_{\text{upper}}(r) = -1.3767r^2 + 1.0743r + 0.1452 \quad (19)$$

$$g_{\text{lower}}(r) = -0.7760r^2 + 0.5601r + 0.1766. \quad (20)$$

Fig. 8 Comparison of different enhancement approaches on a dark scene image using a photoflash. (a) Original image; (b) HE-enhanced image; (c) Picasa software-enhanced image; (d) EC-enhanced image; (e) LCC-enhanced image; (f) SC-enhanced image; and (g) JND-HE-EC-enhanced image.

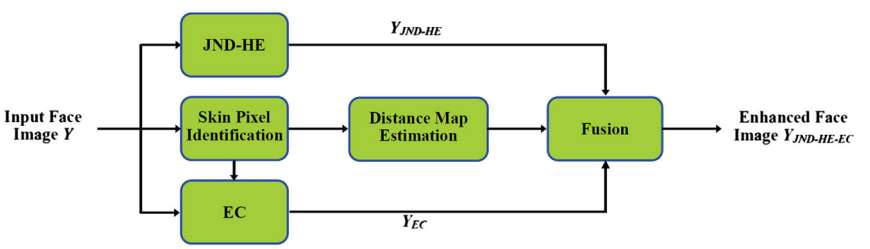

Fig. 9 The flowchart of the proposed JND-HE-EC face image enhancement approach.

A pixel is detected as a skin pixel if its r and g values satisfy the following constraints:

$$0.2 < r < 0.6 \text{ and } g_{\text{lower}}(r) < g < g_{\text{upper}}(r) \text{ and } W > 0.0004, \tag{21}$$

where $W = (r - 0.33)^2 + (g - 0.33)^2$ is provided to prevent from labeling whitish pixels as skin pixels. As a result, a face skin map, denoted by M_{fs}, will be generated to indicate whether a pixel is a face skin pixel [denoted by $M_{\text{fs}}(x, y) = 1$] or not [denoted by $M_{\text{fs}}(x, y) = 0$]. Then, the morphological operation[3] is conducted on the face skin map to eliminate the noises and fill the holes in the face skin map. Figure 10 shows some input images, their detected face regions, and identified face skin pixels. We can see that most face regions and face skin pixels can be correctly detected except for the central face in the rightmost image because its pose is far from upright. Thus, the face detection approach proposed by Viola and Jones[16,17] fails to detect this face region.

3.2 *The EC Method*

The EC method[9] tries to adjust the illumination in an image based on the difference between the average luminance of all reference pixels and the desired luminance value. A simulated camera response curve,[19] showing the relation between a light value q (called "light quantity") and the pixel value I transformed by the camera sensor, was developed to adjust the exposure level. This camera response curve f can be represented by the following equation:

$$I = f(q) = \frac{255}{(1 + e^{-Aq})^C}, \tag{22}$$

where parameters A and C are used to control the shape of the curve. Thus, the original light quantity q can be derived from a reference luminance value using the inverse transformation of the camera response curve f. In this study, the mean luminance value of all face skin pixels was computed as the reference luminance value. First, the average

Fig. 10 Some example images illustrating the results of face detection and skin pixel identification. The upper row shows the test images and the detected face regions; the bottom row shows the identified face skin pixels.

luminance Y_{avg} of all detected face skin pixels is computed. The simulated camera response curve f is then used to measure the light quantity difference between Y_{avg} and a predefined ideal luminance value Y_{ideal}:

$$q_{\text{offset}} = f^{-1}(Y_{\text{ideal}}) - f^{-1}(Y_{\text{avg}}). \tag{23}$$

The luminance value of each pixel can then be modified using the following equation:

$$Y_{\text{EC}}(x,y) = f\left\{ f^{-1}[Y(x,y)] + q_{\text{offset}} \right\} \tag{24}$$

3.3 *Estimation of the Distance Map*

To fuse together the independently enhanced images Y_{EC} and $Y_{\text{JND-HE}}$ into one image, we use a weighted sum of the two images. In this paper, the weight for fusing these two images is based on a distance map, denoted by M_{dist}, which records the distance between each pixel and its nearest face skin pixel. If a pixel located at (x,y) is close to one of the connected face regions, the distance value recorded in the distance map corresponding to the pixel location (x,y), $M_{\text{dist}}(x,y)$, is small. On the other hand, if a pixel is far from any connected face region, a large distance value will be recorded in $M_{\text{dist}}(x,y)$. To construct the distance map, we first use the region growing algorithm [3] to label each connected face region based on the detected face skin map M_{fs}. Let there be S connected face regions in the input image, denoted by $R_{\text{fs},1}$, $R_{\text{fs},2}$, $\ldots$, $R_{\text{fs},S}$. Associated with the ith face region $R_{\text{fs},i}$, $1 \le i \le S$, a corresponding face distance map, denoted by $M_{\text{dist},i}$, will be constructed independently. The overall face distance map M_{dist} can be obtained by fusing all individual face distance maps. For each connected face region $R_{\text{fs},i}$, we iteratively use the morphological dilation operation[3] to estimate $M_{\text{dist},i}$, $1 \le i \le S$. Typically, if a pixel is near a connected face region, it will be dilated earlier. Thus, the iteration number at which the pixel is dilated will be regarded as the face distance between the pixel and a connected face region. For example, if a pixel located at (x,y) is dilated at the tth iteration, set $M_{\text{dist},i}(x,y) = t$. Note that for the same pixel, the face distance values recorded in different connected face regions may be distinct. That is, $M_{\text{dist},i}(x,y) \neq M_{\text{dist},j}(x,y)$ for $i \neq j$. Hence, the overall face distance value, $M_{\text{dist}}(x,y)$, is defined as the minimum among all face distance maps:

$$M_{\text{dist}}(x,y) = \min_{1 \le i \le S} M_{\text{dist},i}(x,y). \tag{25}$$

In this paper, a maximum number of dilation operations, T, will be defined to reduce the computation time. After T iterations, those pixels that are not dilated yet will be assigned a value of $T+1$, indicating that they are too far from any connected face region. A detailed description will be given next.

Notation and initialization: Let t denote the number of the dilation operations performed so far, and initially set $t = 0$. Let $R_{\text{fs},i}$ and $M_{\text{dist},i}$, denote the ith connected face region and the corresponding distance map, respectively. Initially, set $M_{\text{dist},i}(x,y) = 0$ if $M_{\text{fs}}(x,y) = 1$ and $(x,y) \in R_{\text{fs},i}$; otherwise, set $M_{\text{dist},i}(x,y) = T+1$.

Step 1: Set $t = t+1$. Perform the morphological dilation operation on each connected skin region $R_{\text{fs},i}$ using a disk structuring element and set t as the distance values of all pixels dilated at the present iteration, $M_{\text{dist},i}(x,y) = T$.
Step 2: If $t < T$, go to Step 1.
Step 3: Compute the overall distance map M_{dist} using Eq. (25).

It should be noted that the face skin map M_{fs} is scaled down by a factor of 1/4. Thus, the face distance map M_{dist} is also 1/4 the size of the original image. To fuse together the independently enhanced images Y_{EC} and $Y_{\text{JND-HE}}$, the face skin map must be scaled up to the same size as its original. In this paper, a bilinear interpolation by a factor of 4 is used for this purpose.

3.4 *Fusion of the Independently Enhanced Images*

We define the fused luminance value of the pixel located at (x,y), $Y_{\text{JND-HE-EC}}(x,y)$, as a weighted sum of $Y_{\text{EC}}(x,y)$ and $Y_{\text{JND-HE}}(x,y)$, given as

$$\begin{aligned} Y_{\text{JND-HE-EC}}(x,y) = {} & w(x,y) Y_{\text{JND-HE}}(x,y) \\ & + [1 - w(x,y)] Y_{\text{EC}}(x,y), \end{aligned} \tag{26}$$

where the weight value $w(x,y)$ is represented by a power-law function of the distance value $M_{\text{dist}}(x,y)$, given by

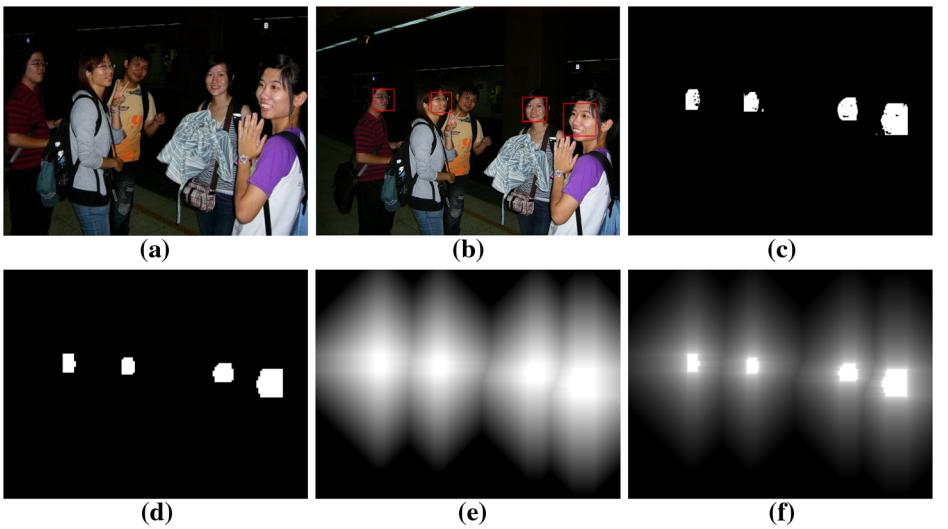

Fig. 11 An example of face region detection, face skin pixel identification, distance map construction, and weighted value evaluation. (a) An input image; (b) detected face regions; (c) a detected face skin map; (d) a morphologically refined face skin map; (e) the distance map with brighter pixels having smaller distance values; and (f) the weight map.

$$w(x,y) = \left[\frac{M_{\text{dist}}(x,y)}{T+1}\right]^{\beta}. \tag{27}$$

Therefore, if $M_{\text{dist}}(x,y)$ is very small, this enhanced value tends to close to $Y_{\text{EC}}(x,y)$. We set the power-law curve with parameter $\beta = 0.4$ in these experiments because such a setting can map a narrow range of distance values into a wider range of weight values. As a result, the boundary regions between face and nonface areas will become sharper and thus will not generate any halo effect. Figure 11 shows an input image as well as the face skin map, distance map, and weight map associated with the input image. Finally, the reconstructed color image can be obtained using Eqs. (16)–(18) by replacing $Y_{\text{JND-HE}}(x,y)$ with $Y_{\text{JND-HE-EC}}(x,y)$.

4 Experimental Results

In this paper, some images with the following problems will be used for performance comparison: (1) overexposed

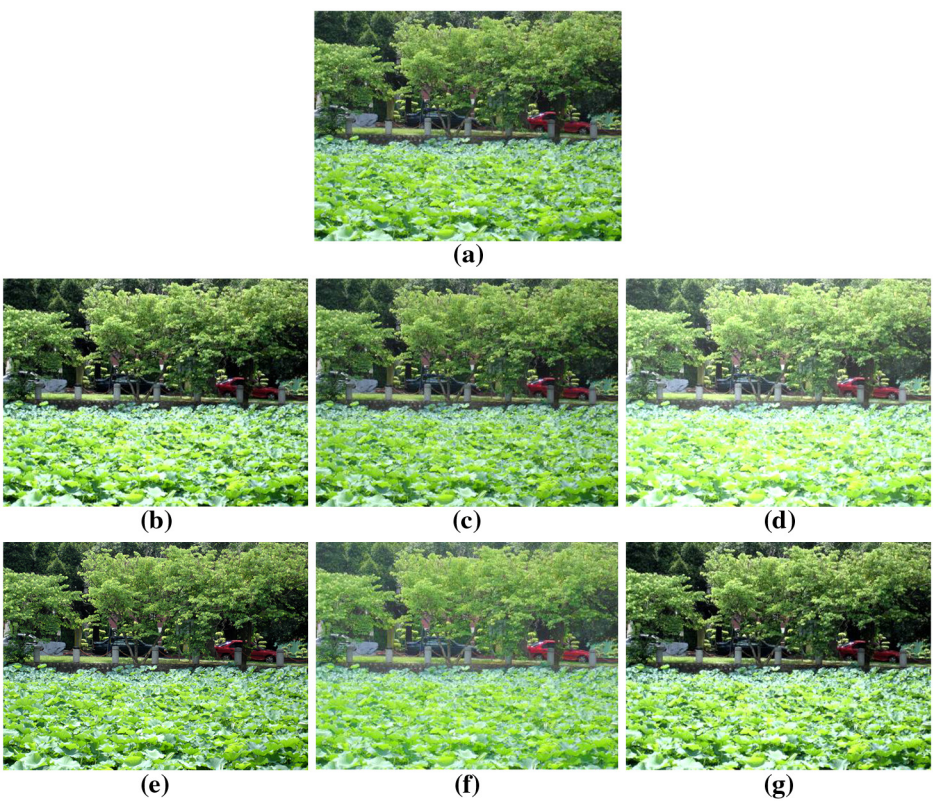

Fig. 12 Comparison of different enhancement approaches on a normal image. (a) Original image; (b) HE-enhanced image; (c) Picasa software—enhanced image; (d) EC-enhanced image; (e) LCC-enhanced image; (f) SC-enhanced image; and (g) JND-HE—enhanced image.

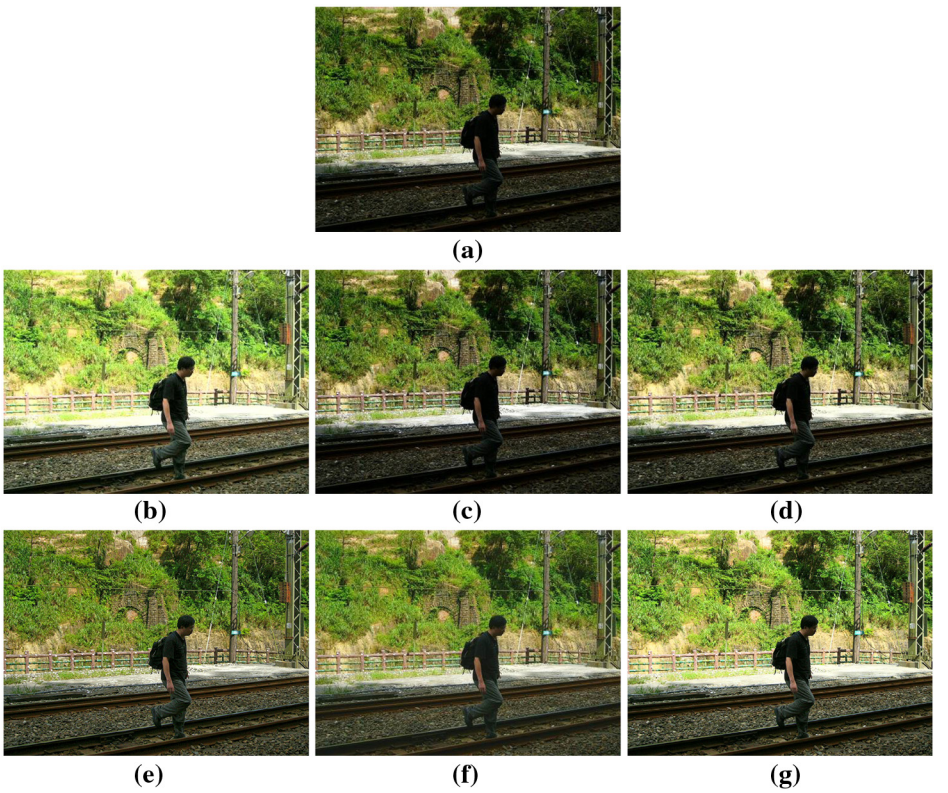

Fig. 13 Comparison of different enhancement approaches on an image with shadow areas. (a) Original image; (b) HE-enhanced image (c) Picasa software—enhanced image; (d) EC-enhanced image; (e) LCC-enhanced image; and (f) SC-enhanced image; (g) JND-HE—enhanced image.

and/or underexposed problems, (2) low-contrast problems, and (3) normal images with proper illumination/exposure. The proposed approach will be compared to some other methods, including (1) HE,[3] (2) Picasa software,[2] (3) Battiato's EC algorithm,[9] (4) Schettini's local gamma correction (LCC) algorithm,[8] and (5) Safonov's shadow correction (SC) algorithm.[10] The comparison of experimental results on generic images, as well as face images, also will be given.

4.1 *Experimental Results on Generic Images*

Four different kinds of generic images, including a normal image, an image with shadow areas, an image taken in a backlight condition, and a dark scene image will be used for performance comparison.

Figure 12(a) shows an original image with proper exposure and the enhanced images obtained using different approaches. We can see that HE yields a sharper image than the original [see Fig. 12(b)]. From Fig. 12(c) and 12(f), we can see that the enhanced images using Picasa software and Safonov's SC algorithm are similar to the original. From Fig. 12(d), we can see that the lotus leave area is overexposed using Battiato's EC algorithm. In Fig. 12(e), the global contrast decreases although the contrast in local regions is appropriate. By comparing all enhanced images, we can see that our JND-HE approach [see Fig. 12(g)] yields a high-contrast image that looks more vivid than the others.

Figure 13 shows an input image with shadow areas and the enhanced images obtained using different approaches. From these images, we can see that our JND-HE approach and HE produced proper contrast and illumination in the shadow areas.

Figure 1 shows an image having both overexposed and underexposed regions, as well as the enhanced images obtained using different approaches. From Fig. 1(b), we can see that HE produces obviously false contours in the overexposed sky area, although the underexposed area (the foreground building) is clearly enhanced. The image enhanced using Picasa software is almost identical to the original [see Fig. 1(c)]. In Fig. 1(d), Battiato's EC algorithm has enhanced the dark area appropriately but lost the detail information in the sky area. Schettini's LCC algorithm and Safonov's SC algorithm can enhance the shadow areas to some extent, but the global contrast is not appealing [see Fig. 1(e) and 1(f)]. In Fig. 1(g), we can see that JND-HE produces proper illumination and high contrast in the foreground building and keeps the details of the sky area.

Figure 2 shows a dark scene and the enhanced images obtained using different approaches. From Fig. 2(b), we can see that HE amplifies the background noises and produces a halo effect near the streetlight. Schettini's LCC algorithm also amplifies the background noises and produces the halo effect near the streetlight to some degree [see Fig. 2(e)]. The improvement of the enhanced images produced by using Picasa software and Safonov's SC algorithm is not clear [see Fig. 2(c) and 2(f)]. Battiato's EC algorithm produces a washed-out appearance and also suffers from an obvious halo effect near the streetlight [see Fig. 2(d)]. Our JND-HE method produces obvious improvement in the dark area without generating any artifacts [see Fig. 2(g)]. Further, we can see that the dark area looks clearer using our JND-HE method.

4.2 *Experimental Results on Face Images*

Typically, the exposure problems that most frequently occur in images with face regions happen in the following situations: (1) the images were taken at night using a photoflash, and (2) the images were taken in backlight conditions. In the first case, the human faces appear clearly, but the background is unclear since the photoflash gives less illumination on the background. In the second case, the human faces are generally dark and unclear due to relatively insufficient illumination in the foreground face regions. In this paper, some images suffering from these problems will be used for performance comparison.

Figure 8 shows a face image with dark background and the enhanced images obtained using different approaches. To improve the illumination in the background region, HE also amplifies the background noises and overexposes the face regions [see Fig. 8(b)]. Picasa software and Battiato's EC algorithm enhance the face regions slightly, but the background is still unclear [see Fig. 8(c) and 8(d)]. From Fig. 8(e), Schettini's LCC algorithm can produce more distinguishable details in the background, but the face regions become unnatural due to insufficient contrast. Safonov's SC algorithm and our JND-HE-EC approach enhance both the background and face regions [see Fig. 8(f) and 8(g)]. However, we can see that the image enhanced using our JND-HE-EC approach yields a clearer background and proper illumination in face regions.

Figure 3 shows a face image taken in backlight conditions and the enhanced images obtained using different approaches. In Fig. 3(b), we can see that HE produces a washed-out appearance in the face region, and thus, the face looks unnatural. The images enhanced using Picasa software, Schettini's LCC algorithm, and Safonov's LC algorithm exhibit insufficient illumination in the face region [see Fig. 3(c), 3(e), and 3(f)]. In Fig. 3(d), we see that Battiato's EC algorithm enhances the face region appropriately but excessively enhances the background. Our JND-HE-EC method provides a clear face and produces an appropriate background as well.

5 Conclusion and Future Work

In this paper, we have proposed automatic and effective contrast enhancement approaches for generic images as well as faces. The JND-HE method, which exploits the JND model of the HVS, is proposed for generic image enhancement. An evaluation function based on the JND model is designed to assess whether HE can be employed directly to enhance an input image without introducing any noticeable distortion or artifacts. To improve face images, we proposed the JND-HE-EC method, which combines our JND-HE approach with Battiato's EC method[9] to obtain an enhanced image that provides appropriate contrast in face regions and proper illumination in background areas. Experimental results on both generic images and faces have shown that our proposed methods produce more pleasingly enhanced images than other methods, such as HE, Picasa software, Battiato's EC algorithm, Schettini's LCC algorithm, and Safonov's SC algorithm.

Based on the experimental results, we can see that the parameter r used in Eq. (6) will affect the quality of the enhanced images to some degree. A smaller r value will produce a higher-contrast image, whereas the background noise is also amplified. On the other hand, a larger r value will attenuate the background noise at the cost of reduced contrast. Thus, a simple pixel-by-pixel averaging of the images enhanced using different r values is employed to provide a better trade-off between low noise and high contrast. In the future, we will try to assign different weights to these images adaptively according to the context and/or contrast analysis on these enhanced images, or by utilizing image fusion techniques[20,21] on these images to produce an image with higher contrast than each individual one.

It can be noted that the JND-HE approach is based only on the luminance values of image pixels, not all color values. Thus, in the near future, we will try to integrate the JND model with the color HE method[22] in order to achieve more appealingly enhanced images.

Acknowledgments

This research was supported in part by the National Science Council, R.O.C., under Contract NSC 98-2221-E-009-117-MY2. The authors would like to thank the anonymous reviewers for their valuable comments that improved the representation and quality of this paper.

References

1. Adobe Systems Inc., "Image editor software-Adobe Photoshop," http://www.adobe.com/products/photoshop.
2. Google, Inc., "Picasa software," http://picasa.google.com.
3. R. C. Gonzalez and R. E. Woods, *Digital Image Processing*, 2d ed., Prentice-Hall, Upper Saddle River, New Jersey (2002).
4. Y. T. Kim, "Contrast enhancement using brightness preserving bi-histogram equalization," *IEEE Trans. Consum. Electron.* **43**(1), 1–8 (1997).
5. Y. Wang, Q. Chen, and B. Zhang, "Image enhancement based on equal area dualistic sub-image histogram equalization method," *IEEE Trans. Consum. Electron.* **45**(1), 68–75 (1999).
6. S. M. Pizer et al., "Adaptive histogram equalization and its variations," *Comp. Vision, Graph. Image Proc.* **39**(3), 355–368 (1987).
7. N. Moroney, "Local colour correction using non-linear masking," in *Proc. IS&T/SID Eighth Color Imaging Conf.*, pp. 108–111, IS&T, Springfield, VA (2000).
8. R. Schettini et al., "Contrast image correction method," *J. Electron. Imag.* **19**(2), 023025 (2010).
9. S. Battiato et al., "Automatic image enhancement by content dependent exposure correction," *EURASIP J. Appl. Sig. Proc.* **2004**(12), 1849–1860 (2004).
10. I. V. Safonov et al., "Automatic correction of exposure problems in photo printer," in *Proc. IEEE Tenth Int. Symp. Consum. Electron.*, pp. 1–6, IEEE, Piscataway, NJ (2006).
11. Z. Y. Chen et al., "A generalized and automatic image contrast enhancement using gray level grouping," in *Proc. IEEE Int. Conf. Acous., Speech, Sig. Proc.*, Vol. 2, pp. 965–968, IEEE, Piscataway, NJ (2006).
12. C. H. Chou and Y. C. Li, "A perceptually tuned subband image coder based on the measure of just-noticeable-distortion profile," *IEEE Trans. Circuits Syst. Video Technol.* **5**(6), 467–476 (1995).
13. S. Sakaue et al., "Adaptive gamma processing of the video cameras for the expansion of the dynamic range," *IEEE Trans. Consum. Electron.* **41**(3), 555–562 (1995).
14. F. Naccari et al., "Natural scenes classification for color enhancement," *IEEE Trans. Consum. Electron.* **51**(1), 234–239 (2005).
15. C. Shi et al., "Automatic image quality improvement for videoconferencing," in *Proc. IEEE Int. Conf. Acous., Speech, Sig. Proc.*, Vol. 3, pp. 701–704, IEEE, Piscataway, NJ (2004).
16. P. Viola and M. Jones, "Rapid object detection using a boosted cascade of simple features," in *Proc. IEEE Conf. Comp. Vision Patt. Recog.*, Kauai, Hawaii, pp. 511–518, IEEE, Piscataway, NJ (2001).
17. P. Viola and M. Jones, "Robust real-time face detection," *Intl. J. Comp. Vis.* **57**(2), 137–154 (2004).
18. M. Soriano et al., "Skin color modeling under varying illumination conditions using the skin locus for selecting training pixels," in *Proc. Workshop Real-time Image Seq. Anal.*, pp. 43–49, Oulu, Finland (2000).
19. S. Battiato, A. Castorina, and M. Mancuso, "High dynamic range imaging for digital still camera: an overview," *J. Elec. Imag.* **12**(3), 459–469 (2003).
20. Z. Wang et al., "A comparative analysis of image fusion methods," *IEEE Trans. Geosci. Remote Sens.* **43**(6), 1391–1402 (2005).
21. G. Pajares and J. M. de la Cruz, "A wavelet-based image fusion tutorial," *Pattern Recogn.* **37**(9), 1855–1872 (2004).

22. E. Pichon, M. Niethammer, and G. Sapiro, "Color histogram equalization through mesh deformation," in *Proc. Int. Conf. Image Proc.*, Vol. 2, pp. 117–120, IEEE, Piscataway, NJ (2003).

Chang-Hsing Lee received his BS and PhD degrees in computer and information science from National Chiao Tung University, Hsinchu, Taiwan, in 1991 and 1995, respectively. He is currently an associate professor in the Department of Computer Science and Information Engineering at Chung Hua University, Hsinchu, Taiwan. His main research interests include audio/music classification, image processing, pattern recognition, and multimedia information retrieval.

Pei-Ying Lin received a BS in computer science and information engineering from National Cheng Kung University, Tainan, Taiwan, in 2005 and an MS at the Institute of Multimedia Engineering from National Chiao Tung University, Hsinchu, Taiwan, in 2007. Since September 2007, she has been working at the Taiwan Semiconductor Manufacturing Company as a digital IC design engineer. Her main research interests include image processing and digital design.

Ling-Hwei Chen received a BS in mathematics and an MS in applied mathematics from National Tsing Hua University, Hsinchu, Taiwan, in 1975 and 1977, respectively, and a PhD in computer engineering from National Chiao Tung University, Hsinchu, Taiwan, in 1987. From 1977 to 1979, she worked as a research assistant at the Chung-Shan Institute of Science and Technology, Taoyan, Taiwan. From 1979 to 1981, she worked as a research associate at the Electronic Research and Service Organization, Industry Technology Research Institute, Hsinchu, Taiwan. From 1981 to 1983, she worked as an engineer in the Institute of Information Industry, Taipei, Taiwan. She is now a professor in the Department of Computer Science at the National Chiao Tung University. Her current research interests include image processing, pattern recognition, multimedia compression, content-based retrieval, and multimedia steganography.

Wei-Kang Wang received a BS in computer science from National Chiao Tung University, Hsinchu, Taiwan, in 2010. He is currently a graduate student at the Institute of Multimedia Engineering, National Chiao Tung University, Hsinchu, Taiwan. His main research interest is image processing.